The effects of trailing edge blowing on aerodynamic characteristics of the naca 0012 airfoil and optimization of the blowing slot geometry

K. Yousefi, R. Saleh

JOURNAL OF THEORETICAL AND APPLIED MECHANICS
52, 1, pp. 165-179, Warsaw 2014

THE EFFECTS OF TRAILING EDGE BLOWING ON AERODYNAMIC CHARACTERISTICS OF THE NACA 0012 AIRFOIL AND OPTIMIZATION OF THE BLOWING SLOT GEOMETRY

Kianoosh Yousefi, Reza Saleh

Islamic Azad University, Mashhad Branch, Department of Mechanical Engineering, Mashhad, Iran

e-mail: kianoosh_py@yahoo.com

The effects of blowing and its parameters including the jet amplitude, blowing coefficient and jet width in order to flow control was evaluated for a NACA 0012 airfoil. The flow was considered as fully turbulent with the Reynolds number of $5 \cdot 10^5$, and the Menter shear stress turbulent model was employed. Tangential and perpendicular blowing at the trailing edge were applied on the airfoil upper surface, and the jet widths were varied from 1.5 to 4 percent of the chord length, and the jet amplitude was also selected 0.1, 0.3 and 0.5. In the tangential blowing, the results showed that when the blowing amplitude increases, the lift-to-drag ratio rises by 15 percent, however, the smaller amounts of the blowing amplitude are more effective in the perpendicular blowing. Furthermore, when the blowing jet width rises, the lift-to-drag ratio increases continuously in the tangential blowing and decreases quasi-linear in the perpendicular blowing. In this study, the blowing jet width 3.5 and 4 percent of the chord length for the tangential blowing was selected as optimal values as well as smaller amounts of blowing jet width are more suitable for the perpendicular blowing. Finally, the lift-to-drag ratio was increased by 17 percent for the tangential blowing in the angle of attack of 18 degrees.

Key words: tangential and perpendicular blowing, blowing jet width, blowing amplitude, lift and drag coefficients, flow control

1. Introduction

Although potential theory can be used to explain many aerodynamics phenomena, there are cases in which the boundary layer significantly alters theoretical predictions. A simple example is the flow past an airfoil. At low angles of attack, the streamline pattern about such a shape is very close to the predictions of inviscid theory. However, a drag force not accounted for by such a theory exists. This drag is largely due to viscous shear forces and is called skin-friction drag. In regions over the surface, in which the boundary layer flow is laminar, the fluid mixing and viscous skin friction are low. However, such laminar flows are often unstable and develop into turbulent flows. Turbulent flows involve more rapid mixing, which produces higher skin-friction drag. On occasion, a combined action of viscous forces and an adverse pressure gradient produces a reversal of the flow next to the surface which, in turn, causes separation of the adjacent flow from the surface. The presence of the boundary layer has produced many design problems in all areas of fluid mechanics. However, the most intensive investigations have been directed towards its effect upon the lift and drag of wings. The technique that have been developed to manipulate the boundary layer, either to increase the lift or decrease the drag, are classified under the general heading of boundary layer control or flow control (Hazen, 1967). Another definition of this topic was offered by Flatt (1961). According to his considerations, boundary layer control includes any mechanism or process in which the boundary layer of a fluid flow is caused to behave differently than it normally would, where the flow develops naturally along a smooth straight surface. Methods of flow control to achieve transition delay, separation postponement, lift enhancement,

drag reduction, turbulence augmentation and noise suppression were considered by Gad-el-hak (2000).

One of the most favorable classification schemes of flow control methods considers energy expenditure and control loops involved. As shown in the schematic in Fig. 1, a control device can be passive, requiring no auxiliary power and no control loop, or active, requiring energy expenditure. Normal uniform suction and blowing, which is among passive flow separation control, has been considered in recent years, and most of studies have been focused on oscillatory suction or blowing near the leading edge. However, the effects of variation of suction and blowing parameters, which could provide a suitable research area, has not been considered appropriately.

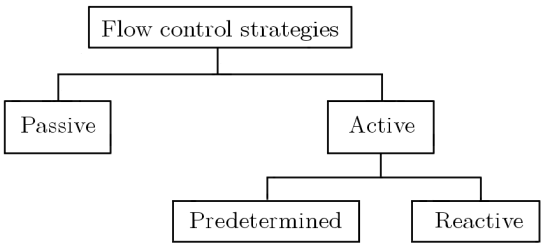

Fig. 1. Classification of flow control strategies

Many studies have been conducted on flow control approaches. Prandtl (Schlichting, 1968) was the first scientist who employed boundary layer suction on a cylindrical surface to delay boundary layer separation. The efficiency of tangential unsteady suction and blowing in flow control for the TAU0015 airfoil was studied by Ravindran (1999). He also evaluated the effects of Zero Net Mass Flux Oscillatory Jet (Synthetic Jet) on the lift coefficient, and the lift coefficient was increased about 23 and 55 percent in angles of attack of 22 and 24 degrees, respectively. Guowei *et al.* (1997) numerically studied the effects of leading edge blowing-suction on the vortex flow past an airfoil at high incidence. The results indicated that the frequency of the flow field excited by periodic blowing-suction locks into the forcing frequency, which is half of the dominant frequency for the flow past a fixed airfoil without injection. In that case, a wall developed primary leading edge vortex occupies the upper surface of the airfoil, and the largest lift augmentation is obtained. Huang *et al.* (2004) investigated the suction and blowing flow control approaches for the NACA 0012 airfoil. When the jet location and angle of attack were combined, perpendicular suction at the leading edge from 0.075 to 0.125 of the chord length, has increased the lift coefficient better than other suction situations. It was also found that tangential blowing at downstream locations, around 0.371 to 0.8 of the chord length, leads to the maximum increase in the lift coefficient value. Rosas (2005) numerically investigated the flow control over the NACA 0015 airfoil by oscillatory fluid injection and the results demonstrated that the maximum increase in the mean lift coefficient of 93 percent was predicted by the code. Flow separation control by synthetic jets on the NACA 0015 airfoil by using the Large Eddy Simulation method was done by You and Moin (2008). The outcomes presented that the lift coefficient increased by 70 percent and the drag coefficient decreased by 18 percent while flow control parameters were changed. Numerical simulations for the aerodynamic analysis of a two-dimensional airfoil were carried out to increase the efficiency of the circulation control system by Jensch *et al.* (2010).

Varied slot heights at different flap deflection angles as well as leading edge blowing have been investigated to optimize the high lift performance of the airfoil. The numerical simulations for an airfoil using a second blowing slot at the leading edge demonstrated that the additional blowing prevents the occurrence of a thin separation bubble near the leading edge. Genc *et al.* (2011) studied the numerical effects of suction and blowing on the NACA 2415 airfoil at the transition zone. Although separation bubbles were not entirely eliminated in suction and

blowing simulation, they either reduced or moved into the downstream. For synchronic suction and blowing, the separation bubbles were exterminated completely, the lift coefficient increased and drag coefficient decreased.

Sahu and Patnaik (2011) attached a rotating element in form of an actuator disc, which was embedded on the leading edge of the NACA 0012 airfoil, to inject momentum into the wake region in order to achieve high-performance aerofoils that enable delayed stall conditions and achieve high lift-to-drag ratios. The actuator disc is rotated at different angular speeds for angles of attack between 0 and 240 degrees. A delayed stall angle resulted with an attendant increase in the maximum lift coefficient. Due to delay and/or prevention of separation, the drag coefficient is also reduced considerably, resulting in a high-performance lifting surface. In addition, Yousefi *et al.* (2012) reviewed the recent investigations about common techniques in suction and blowing systems to increase or decrease the drag and lift coefficient. Also some researchers, analytically (Glauert, 1947), experimentally (Dirlik *et al.*, 1992; Mashud and Hossain, 2010) and some numerically (Nae, 1998; Rizzetta *et al.*, 1999; Yousefi *et al.*, 2013a,b) showed that using flow control, such as by blowing and synthetic jets, causes the larger lift coefficient on thick and NACA airfoils.

2. Governing equations

The fluid flow was assumed as steady, incompressible, turbulent and two-dimensional. Therefore, the governing equations for mass and momentum conservation are as follows

$$\frac{\partial \overline{u}_i}{\partial x_i} = 0 \qquad \frac{\partial}{\partial x_j}(\overline{u_i u_j}) = -\frac{1}{\rho}\frac{\partial \overline{P}}{\partial x_i} + \frac{\partial}{\partial x_j}\Big(\nu \frac{\partial \overline{u}_i}{\partial x_j} - \overline{u_i' u_j'}\Big) \tag{2.1}$$

where ρ is density, $\overline{P}$ is mean pressure, ν is kinematic viscosity and $\overline{u}$ refers to mean velocity. The term of $-\overline{u_i' u_j'}$ is the Reynolds stresses tensor that incorporates the effects of turbulent fluctuations. The Reynolds stresses are modeled via the Boussinesq approximation in which the deviatoric part is taken to be proportional to the strain rate tensor through the turbulent viscosity. The incompressible form of the Boussinesq approximation is

$$\overline{u_i' u_j'} = \nu_t\Big(\frac{\partial \overline{u}_i}{\partial x_j} + \frac{\partial \overline{u}_j}{\partial x_i}\Big) - \frac{2}{3}k\delta_i j \tag{2.2}$$

In the above equation, ν_t is the turbulent viscosity, k is the average kinetic energy of the velocity fluctuations and δ_{ij} is the Kronecker delta. Therefore, in order to simulate the turbulent flow, eddy or turbulent viscosity distribution is employed rather than Reynolds stress tensor through the eddy viscosity turbulent models such as algebraic or zero-equation models, one-equation models, two-equation models, etc.

The Menter shear stress transport two-equation model $(k-\omega\text{SST})$ was employed to solve the turbulence equations. This model includes both $k-\omega$ and $k-\varepsilon$ standard models, which improved the calculations of boundary layer flows with separation and removed the sensitivity of $k-\omega$ model in external flows. The transport equations in Menter's shear stress turbulence model are

$$\begin{aligned}
&\frac{\partial}{\partial x_i}(\rho U_i k) = \widetilde{P}_k - \beta^* \rho k\omega + \frac{\partial}{\partial x_i}\Big[(\mu + \sigma_k \mu_t)\frac{\partial k}{\partial x_i}\Big] \\
&\frac{\partial}{\partial x_i}(\rho U_i \omega) = \alpha \rho S^2 - \beta \rho \omega^2 + \frac{\partial}{\partial x_i}\Big[(\mu + \sigma_\omega \mu_t)\frac{\partial \omega}{\partial x_i}\Big] + 2(1-F_1)\rho\sigma_{w2}\frac{1}{\omega}\frac{\partial k}{\partial x_i}\frac{\partial \omega}{\partial x_i}
\end{aligned} \tag{2.3}$$

In these equations, F_1 is the blending function, S is the invariant measure of the strain rate, β^* is 0.09 and σ_{w2} is 0.856. The blending function is equal to zero away from the surface

($k-\varepsilon$ model), and switches over to one inside the boundary layer ($k-\omega$ model). A production limiter $\widetilde{P}_k$ is used in Menter's shear stress transport turbulence model to prevent the build-up of the turbulence in stagnation regions. In addition, it is important to note that all constants are computed by a blend from the corresponding constant of $k-\varepsilon$ and $k-\omega$ models via α, σ_k, σ_ω, etc. (Menter *et al.*, 2003).

3. Numerical simulation

3.1. Parameters selection

The numerical code was performed for all present computations. The code is based on a finite volume computational procedure. Calculations were applied over the NACA 0012 airfoil with one meter chord length and the chord Reynolds number of $5\cdot10^5$. The NACA 0012 section, blowing jet location L_j, blowing angle θ and blowing jet width h are shown in Fig. 2. A previous

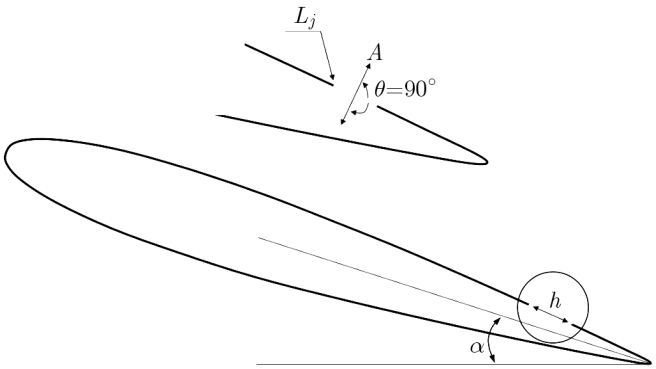

Fig. 2. Blowing parameters

study by Huang *et al.* (2004) showed that the blowing jet location is optimum in two distances on the NACA 0012 airfoil surface, one around 37.1 percent and the other around 80 percent of the chord length from the leading edge. Moreover, recent investigations (Huang *et al.*, 2004; Rosas, 2005) indicated that the blowing jet at the trailing edge is more appropriate rather than other situations. Hence, in this work the blowing jet was considered at 80 percent of the chord length from the leading edge. The blowing jet width was 3.5 percent of the chord length in the tangential and perpendicular blowing and also the blowing amplitude (the blowing velocity to free stream velocity ratio) considered as 0.1, 0.3 and 0.5. Furthermore, the angles of attack of 12, 14, 16 and 18 degrees were applied. The blowing amplitude and blowing jet velocity are defined as

$$A=\frac{u_j}{u_\infty} \qquad u=A\cos(\theta+\beta) \qquad v=A\sin(\theta+\beta) \tag{3.1}$$

where β is the angle between the free stream velocity direction and the local jet surface, and θ is also the angle between the local jet surface and jet output velocity direction. Note that negative θ represents suction condition and positive θ indicates blowing condition. Since the tangential and perpendicular blowing is investigated, θ is 90 and 0 degrees. Finally, the blowing coefficient equals

$$C_\mu=\frac{\rho h v_j^2}{\rho C u_\infty^2}=\frac{h}{C}\frac{u_j^2}{u_\infty^2} \qquad H=\frac{h}{C} \qquad C_\mu=HA^2 \tag{3.2}$$

As it is presented in Eq. $(3.2)_3$, the blowing coefficient depends on two factors, the blowing amplitude A and the non-dimensional blowing jet width H. On the other hand, variation of

those values causes changes in the blowing coefficient value. Over 350 numerical simulations have been performed to cover all the cases.

3.2. Numerical solution method

The first and second order upwind method was employed to discretize the governing equations. First, the equations were discretized by the use of the first-order upwind method, and the resulting system of equations was then solved using the SIMPLE method. The solution procedure was terminated when the convergence criterion of $O(5)$ reduction in all dependent variable residuals was satisfied. Afterwards, the second-order upwind method was employed to discretize the equations and again, the SIMPLE method was applied to solve them. Convergence accuracy at this step was to the extent in which the lift and drag coefficients fully converged, which happened usually at $O(7)$. It is noticeable that the results obtained from the first-order upwind method were used as the initial assumption for the second-order upwind method. It is an attempt to consider the characteristics of a laboratory wind tunnel, so the stream turbulence intensity was considered less than 0.1 percent. The airfoil computational area (C-type structured grid) was generated as multizonal blocks in order to provide a structured mesh, as it is shown in Fig. 3. The computational grid area extends from $-4C$ upstream to $11C$ downstream and the upper and lower boundary extends $4C$ from the profile. The velocity inlet boundary conditions are used with a uniform velocity, $u = 7.3037\cos\theta$, $v = 7.3037\sin\theta$ for the enter and bottom boundaries. Also the outflow boundary conditions are selected for the top and exit boundaries, $\partial u/\partial x = 0$ and $\partial v/\partial x = 0$. To examine independence of the grid, the lift and drag coefficients have been studied for the angle of attack of 16 degrees with different size grids. Table 1 presents the lift and drag coefficients for the angle of attack of 16 degrees and, as it is observed, the grid size of 40600 cells was found to be adequate and economical with good comparison against the experimental results.

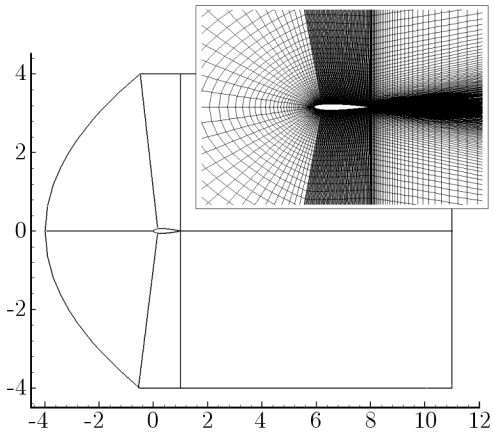

Fig. 3. C-type structured mesh with multizonal blocks

As demonstrated in Figs. 4a and 4b, all simulations were continued until the lift and drag coefficients were reached to ful convergence. Then, the results were compared with the results of the numerical solution by Huang *et al.* (2004) and experimental values by Critzos *et al.* (1955) and Jacobs and Sherman (1937). Huang *et al.* (2004) investigated suction and blowing flow control for the NACA 0012 airfoil whoose angle of attack and the Reynolds number were 18 degree and $5 \cdot 10^5$, respectively. The parameters like jet location, suction and blowing amplitude and angle of attack were also examined by numerical method. In order to model the suction, a jet with 2.5 percent of the chord length as width was placed on the upper surface of the airfoil. The GHOST code, based on finite volume, was used in this study. Critzos *et al.* (1955) examined aerodynamic characteristics of the NACA 0012 airfoil in laboratory experiments, in which the

Table 1. Grid independence study for the NACA 0012 airfoil at the angle of attack of 16 degree and the Reynolds number of $5 \cdot 10^5$

Number of cells	Lift coefficient C_L	Drag coefficient C_D
8096	0.64594	0.20889
17160	1.05134	0.12544
24480	1.09073	0.11567
40640	1.12352	0.10938
58080	1.12319	0.11187

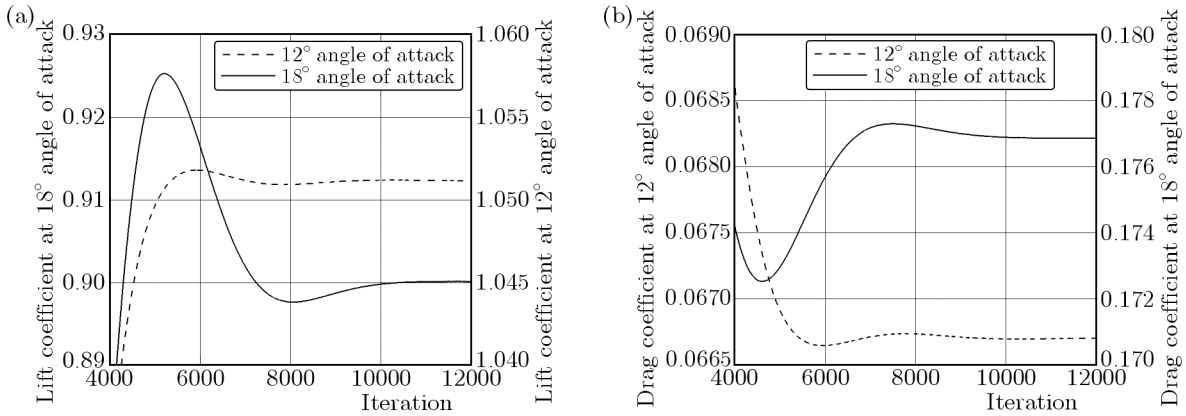

Fig. 4. Convergence history of the lift coefficient (a) and of the drag coefficient (b) for the NACA 0012 airfoil at the Reynolds number of $5 \cdot 10^5$

Reynolds numbers were $0.5 \cdot 10^6$ and $1.8 \cdot 10^6$ as well as the angles of attack varied from 0 to 180 degree. Jacobs and Sherman (1937) investigated symmetrically NACA airfoils in the wind tunnel over a wide range of the Reynolds numbers. The results of all abovementioned solutions are compared in Fig. 5. As it is seen, the computation results are near the numerical simulation by Huang *et al.* (2004) and experimental data by Jacobs and Sherman (1937). The highest

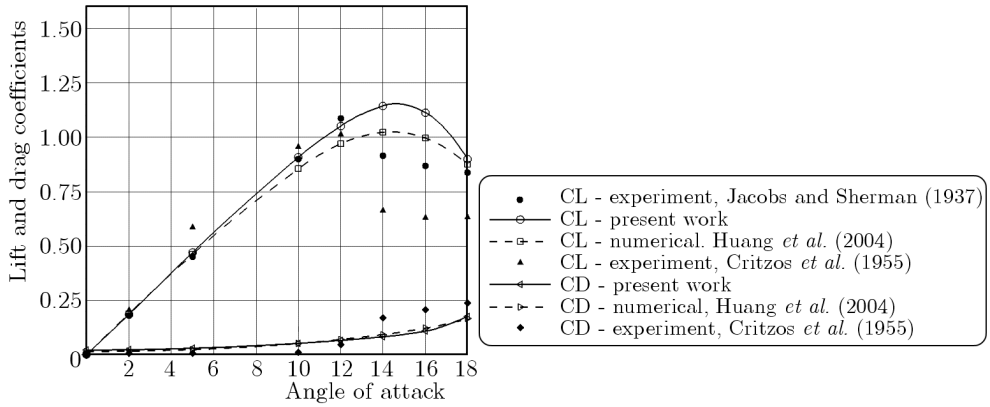

Fig. 5. Comparison between computation results with the numerical work by Huang *et al.* (2004) and experimental results by Critzos *et al.* (1955) and Jacobs and Sherman (1937)

recorded error was 8 percent at the angle of attack of 14 degrees for the numerical simulation and 15 percent for the experimental data by Jacobs and Sherman (1937). Also the stall angles in both works were angles of attack of 14 degrees. However, the results of laboratory measurements indicated that the NACA 0012 airfoil stall occurs at about 12 degrees of the angle of attack.

We have compared our computation results at a low angle of attack (less than 10 degree) with the experimental data (Jacobs and Sherman, 1937; Critzos *et al.*, 1955; Sheldhal and Klimas, 1981) in Table 2 (all experimental data at the Reynolds number of $5 \cdot 10^5$). It can be seen that most of all the experimental data are higher than the computational results. The reason can be attributed to the closer wall effects in the experiment, which lead to the increase of the lift. It is also important that selection of the turbulence model has a significant influence on stall prediction. So, the selection of $K - \varepsilon$ realizable model at the same condition changes the stall angle to 16 degrees. Menter's shear stress transport turbulence model had better stall prediction capability than $K - \varepsilon$ two-equation model. Prediction by $K - \varepsilon$ realizable model was quite good in the pre-stall region, while it failed to predict both the stall condition and post-stall phenomena accurately. In $K - \varepsilon$ realizable model, the maximum errors at the angle of attack of 14 degrees for the lift and drag coefficients were 17 percent and 25 percent, respectively.

Table 2. Comparison of computation results and experimental at angles of attack less than 10 degree

Angle of attack	Computation results	Experiment (Critzos *et al.*, 1955)	Experiment (Jacobs and Sherman, 1937)	Experiment (Sheldahl and Klimas, 1981)
0°	0.0021	0	0	0
2°	0.1853	0.2053	0.1807	0.22
5°	0.4715	0.5855	0.4511	0.55
10°	0.9087	0.9542	0.9019	1.003

4. Results and discussion

4.1. Tangential blowing

First, the effects of blowing amplitude and coefficient on the lift and drag coefficients were analyzed in Figs. 6a and 6b for the tangential blowing. The blowing jet width is fixed at 2.5 percent of the chord length. In these figures, three blowing amplitudes 0.1, 0.3 and 0.5 have been considered with the blowing coefficients 0.00025, 0.00225 and 0.00625. As the blowing coefficient rises, the lift coefficient increases marginally and the drag coefficient increases by the angle of attack of 16 degrees, then decreases. Generally, the blowing in the trailing edge improves the drag force. The blowing at angles of attack less than 10 degrees have a negligible effect on the

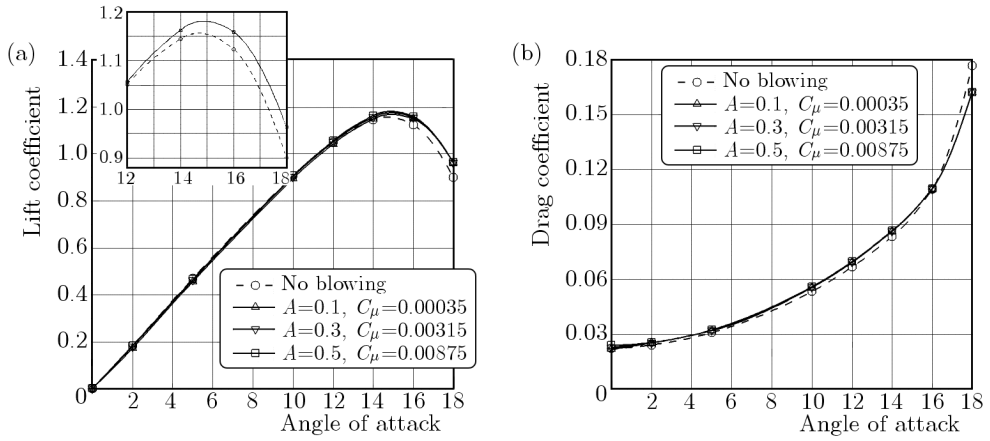

Fig. 6. Effect of the blowing amplitude and blowing coefficient on the lift coefficient (a) and on the drag coefficient (b) for the tangential blowing on the trailing edge

lift and drag coefficients, therefore, in this angle (10 degrees), with the blowing coefficient of 0.00625, the lift coefficient is nearly constant and the drag coefficient rises by 5 percent, while the lift-to-drag ratio decreases about 4.5 percent, which provides an undesirable situation. For this reason, only blowing effects in large angles of attack are taken into account. The largest increase in the lift-to-drag ratio occurs when the blowing coefficient is 0.00625. With the angle of attack of 18 degrees, it rises by about 15 percent. In this case, the lift coefficient rises by 7 percent, while the drag coefficient decreases by 7.5 percent. The interesting thing about the tangential uniform blowing in the trailing edge is that the changes in the blowing amplitude or blowing coefficient have very little effects on the lift and drag coefficients, so that while the blowing amplitude increases from 0.1 to 0.3, and then to 0.5, the lift and drag coefficients remain fixed. This was already shown by Huang *et al.* (2004) for the tangential uniform blowing near the leading edge and in a distance of 0.371. Therefore, unlike in suction, in the blowing (Huang *et al.*, 2004; Goodarzi *et al.*, 2012), the lift and drag coefficients are fixed when the blowing amplitude increases. Moreover, it is worth mentioning that when the blowing coefficient rises, the stall angle stays constant (stall occurs at the same angle of attack of 14 degrees), while the stall occurs slower. In airfoils, it is attempted to prevent from sudden changes in the lift coefficient after stall (sudden stall). The airfoils with thicknesses 6 to 10 percent of the chord length usually have sudden stall, and those with thickness of more than 14 percent of the chord length have gradual stall (Abbott and Von Doenhoff, 1959; Eppler, 1990; Olejniczak and Lyrintzis, 1994). In Fig. 7, also streamlines around the airfoil with the angle of attack of 18 degrees and different blowing coefficients are shown. As can be seen, with the blowing coefficient increased, the vortexes formed behind the airfoil decrease but do not remove.

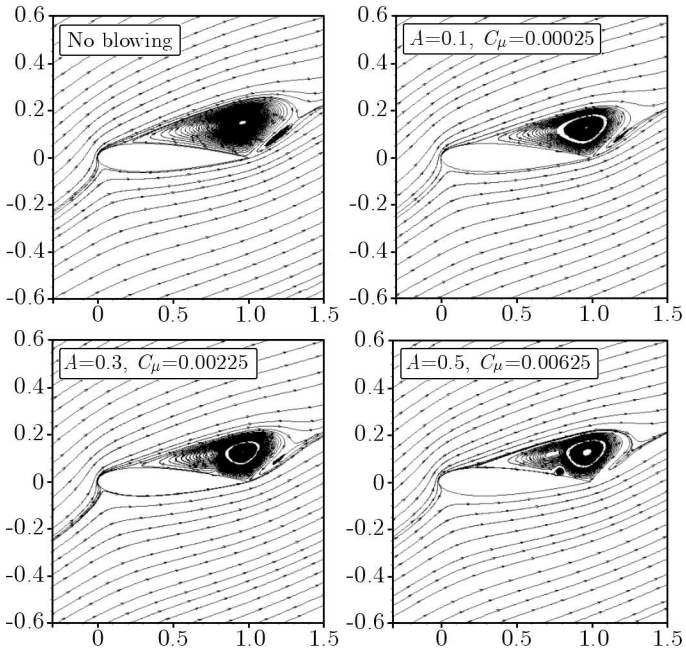

Fig. 7. Streamlines around the airfoil with angle of attack of 18 degrees and different blowing coefficients for the tangential uniform blowing on the trailing edge

Then, the effects of blowing jet width on the lift and drag coefficients for the tangential uniform blowing in the trailing edge will be analyzed. In Figs. 8 and 9, changes of the lift coefficient, drag coefficient, and lift-to-drag ratio are shown with the blowing jet width and blowing amplitude of 0.3 and 0.5. As seen, by an increase in the blowing jet width, the lift coefficient improves and the drag coefficient declines gradually. With the angle of attack of 14 degrees and the blowing amplitude of 0.5, the lift coefficient increases from 1.15658 for

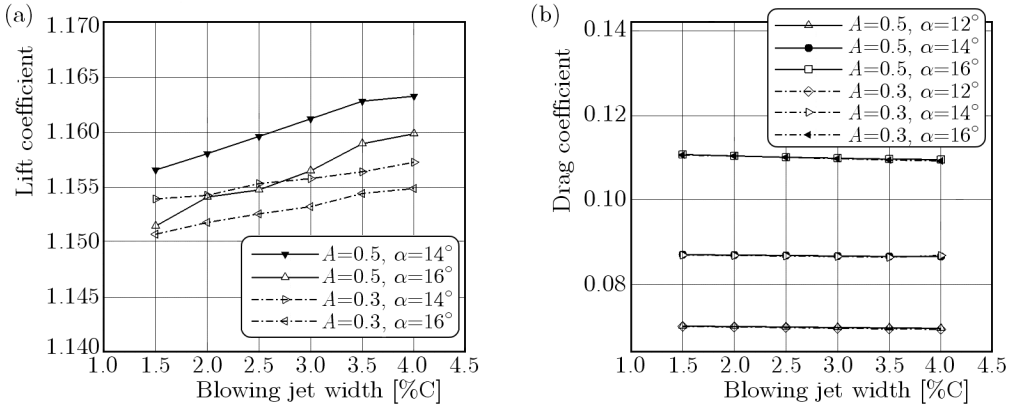

Fig. 8. Changes of the lift coefficient (a) and of the drag coefficient with blowing jet width and blowing amplitude of 0.3 and 0.5 for the tangential blowing

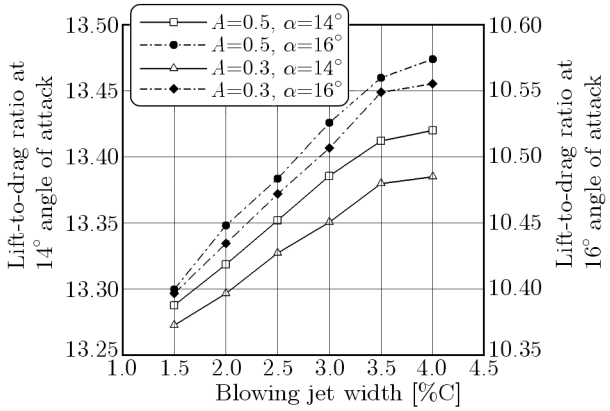

Fig. 9. Changes of the lift-to-drag ratio with blowing jet width for the tangential uniform blowing

the blowing jet width of 1.5 percent to 1.16328 for the blowing jet width of 4 percent of the chord length. Therefore, the lift coefficient rises about one percent, while a decrease in the drag coefficient within this limit is less than 0.5 percent and stays approximately constant. The least increase in the lift coefficient occurs during change in the blowing jet width from 3.5 to 4 percent of the chord length, and generally, the increasing slope of the lift coefficient through blowing jet width 3.5 percent is approximately fixed, and then reduces. On the other hand, the drag coefficient decreases linearly as the blowing jet width increases. This applies for the lift-to-drag ratio: as the blowing jet width increases, the lift-to-drag ratio increases, and the most increase occurs in the angle of attack of 16 degree and is about 2 percent. In addition, note that in the studies conducted on the tangential blowing in the trailing edge, no maximum or minimum in the lift coefficient, drag coefficient, and lift-to-drag ratio are seen. As the blowing jet width increases, the lift coefficient increases; drag coefficient decreases; and lift-to-drag ratio increases as well. The vortexes around the blowing slot move towards downstream, since the blowing in the trailing edge is tangential. As shown in Fig. 10, with the tangential blowing jet width increased, more vortexes are transferred to the downstream. Thus, as the blowing jet width rises, the lift-to-drag coefficient increases continuously, while the blowing jet width either decreases up to 3.5 to 4 percent of the chord length or remains constant. Hence, the best blowing jet width can be considered to be 3.5 to 4 percent. Another interesting point is that the drag coefficient remains constant for different blowing amplitudes. As the blowing amplitude increases, the drag coefficient does not change, the lift coefficient increases as well as the lift-to-drag ratio increases. Generally, the strongest effect of change in the parameters of the tangential blowing in the

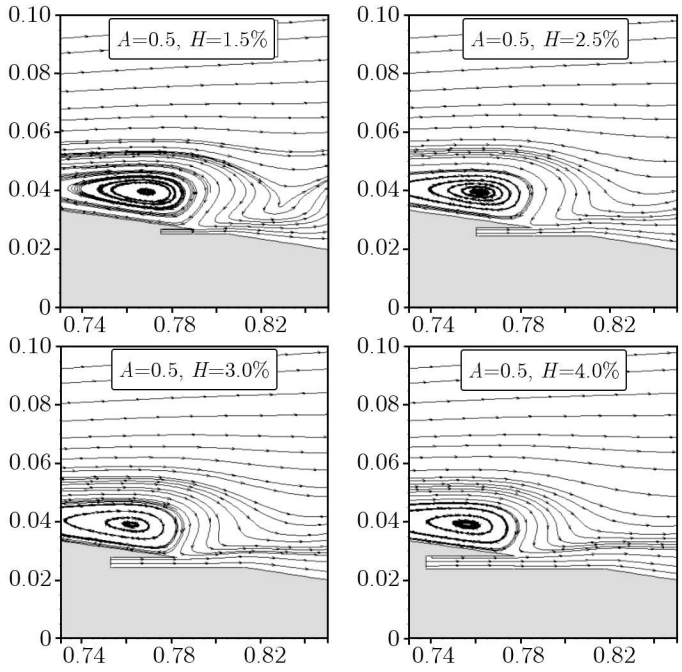

Fig. 10. Streamlines around the blowing slot for the angle of attack of 16 degrees for the tangential uniform blowing

trailing edge is on the lift coefficient, and has little effect on the drag coefficient. As mentioned in the previous Section, the effect of blowing amplitude is very low and increases the lift-to-drag ratio by about 2 percent. Finally, we could increase the lift-to-drag ratio by 17 percent under conditions of the blowing amplitude of 0.5 of the blowing jet width of 4 percent of the chord length and the angle of attack of 18 degrees. In Fig. 11, the effect of blowing jet width on the vortexes behind the airfoil in angle of attack of 16 degrees is shown. For the blowing jet width 3.5 and 4 percent of the chord length, the vortexes formed behind the airfoil decreased.

4.2. Perpendicular blowing

In the final Section, we analyze the uniform perpendicular blowing in the trailing edge as well as the parameters affecting it. In Figs. 12 and 13, the variations of the lift coefficient, drag coefficient, and lift-to-drag ratio with blowing jet width and blowing amplitudes of 0.3 and 0.5 are illustrated. Unlike the tangential blowing, in the perpendicular blowing, the lift coefficient, drag coefficient as well as lift-to-drag ratio decrease continuously with the blowing jet width increase, hence, for the angle of attack of 14 degrees and blowing amplitude of 0.5, the lift coefficient and drag coefficient decreased by about 23 and 16 percent, respectively, when the blowing jet width changed from 1.5 to 4 percent of the chord length. Under these conditions, the lift-to-drag ratio decreases 7 and 3.5 percent for angles of attack of 14 and 16 degrees, respectively. Interestingly, in all the cases studied for the perpendicular blowing, the decrease of the lift and drag coefficients is almost linear and with a constant slope. Moreover, the effect of increased amplitude is much more noticeable in the perpendicular blowing, but this increased blowing amplitude worsens the situation. In the perpendicular blowing with amplitude changed from 0.3 to 0.5, the lift coefficient and lift-to-drag ratio decrease by 10 and 4 percent, respectively, while in the tangential blowing, any increase in the blowing amplitude causes the lift coefficient to rise by one percent and the lift-to-drag ratio by about 2 percent. Generally, the blowing increases boundary layer momentum (Seifert *et al.*, 1996). While adding energy to the boundary layer, the perpendicular blowing increases flow turbulence. Therefore, for greater blowing jet width or

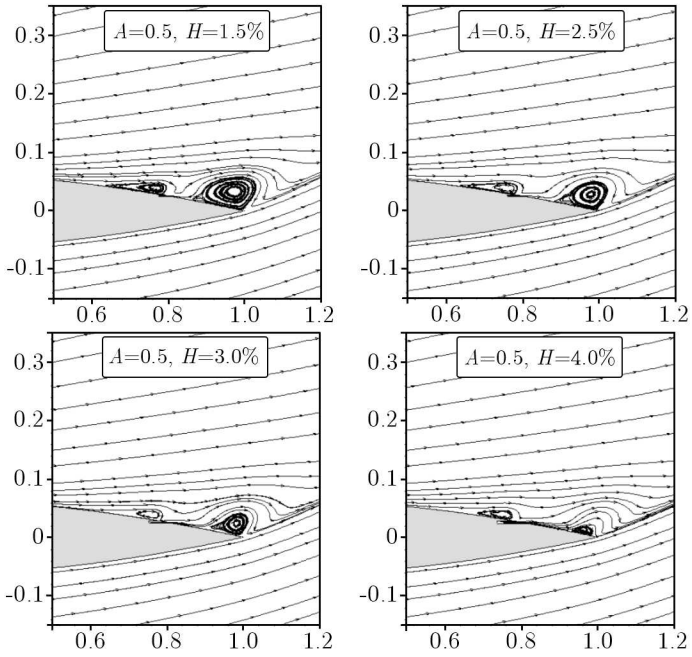

Fig. 11. Effect of blowing jet width on vortexes behind the airfoil for the angle of attack 16° for the tangential uniform blowing

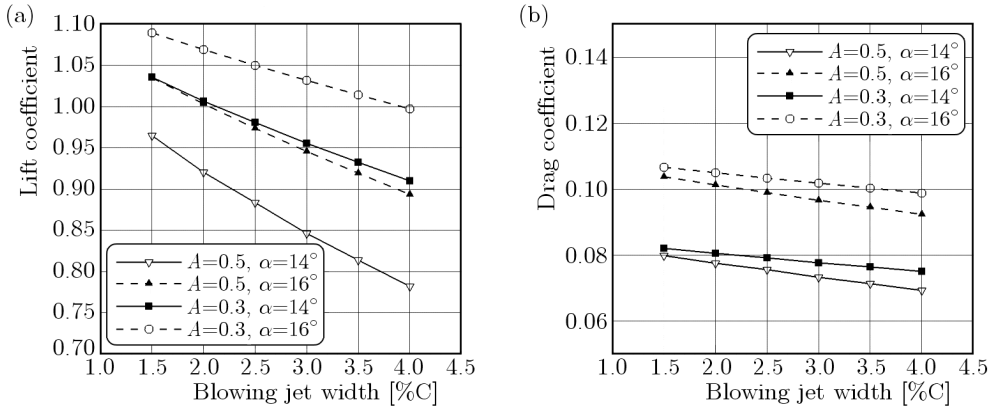

Fig. 12. Changes of the lift coefficient (a) and of the drag coefficient (b) with blowing jet width for blowing amplitude of 0.3 and 0.5 for perpendicular blowing

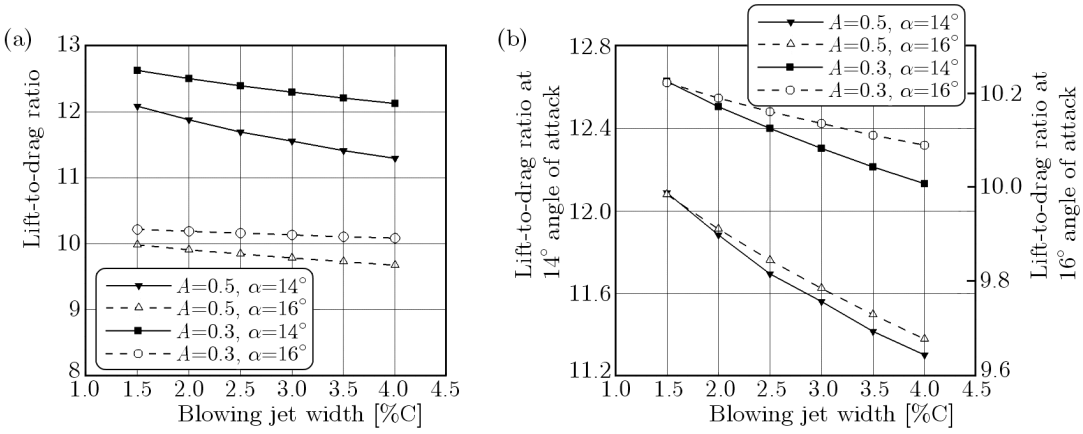

Fig. 13. Changes of the lift-to-drag ratio with blowing jet width for blowing amplitude of 0.3 and 0.5 (a) and for blowing amplitude of 0.3 and 0.5 (b), on a smaller scale, for the perpendicular uniform blowing

blowing amplitude, more eddies become larger and, finally, the lift-to-drag ratio decreases. In Fig. 14, the tangential and perpendicular uniform blowing are compared together for the angle of attack of 16 degrees and blowing amplitude of 0.5. As seen, the perpendicular blowing in the

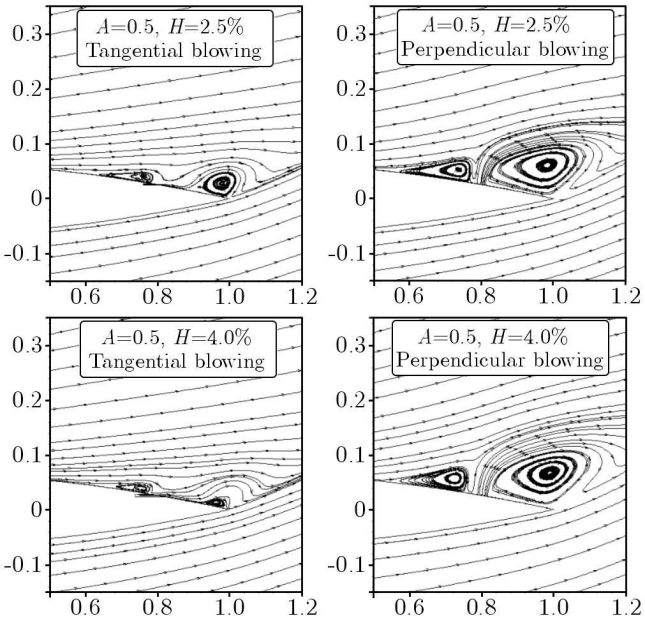

Fig. 14. Comparison between the tangential and perpendicular blowing for the angle of attack of 16 degree

trailing edge causes the eddies to become larger compared with the tangential blowing. Note that, however, the use of the perpendicular blowing also worsens the situation compared with no blowing (until before stall angle); the lift-to-drag ratio for the angle of attack of 14 degrees decrease by 8.7 percent and for the angle of attack of 16 degrees by about 0.5 percent. However, the important thing observed in the perpendicular blowing is that as the angle of attack rises, the effectiveness of the perpendicular blowing increases so that for the angle of attack of 18 degrees, it increases the lift-to-drag ratio by 15 percent. These changes are shown in Table 3.

Table 3. Changes of the lift-to-drag ratio for different angles of attack for the perpendicular uniform blowing in the trailing edge

Angle of attack	Lift coefficient	Drag coefficient	A
10°	0.74506	0.05212	22.5% decrease
12°	0.90386	0.06510	11.2% decrease
14°	1.03606	0.08203	8.71% decrease
16°	1.08956	0.10658	0.53% decrease
18°	0.95585	0.16004	14.8% increase
20°	0.68996	0.27969	2.01% increase

A – Percent of increase/decrease of lift-to-drag ratio compared with the situation without blowing

In Fig. 15, the vectors of amplitude over the airfoil surface in the tangential and perpendicular uniform blowing are compared. The vectors of amplitude were plotted under the conditions of blowing jet width of 4 percent of the chord length; blowing amplitude of 0.5; and angle of attack of 16 degrees. As shown, the tangential blowing postpones separation more than the perpendicular blowing. Separation in the tangential blowing occurs at a distance 0.535 from the

leading edge, while in the perpendicular blowing it occurs at 0.46 from the leading edge. It is also worth mentioning that the perpendicular blowing improves the stall angle from 14 to 16 degree. Finally, the perpendicular blowing improves the stall angle and increases the lift-to-drag ratio for the angles of attack larger than the stall angle. Furthermore, we indicated that a smaller blowing jet width and blowing amplitude provide more effective conditions for using the perpendicular blowing.

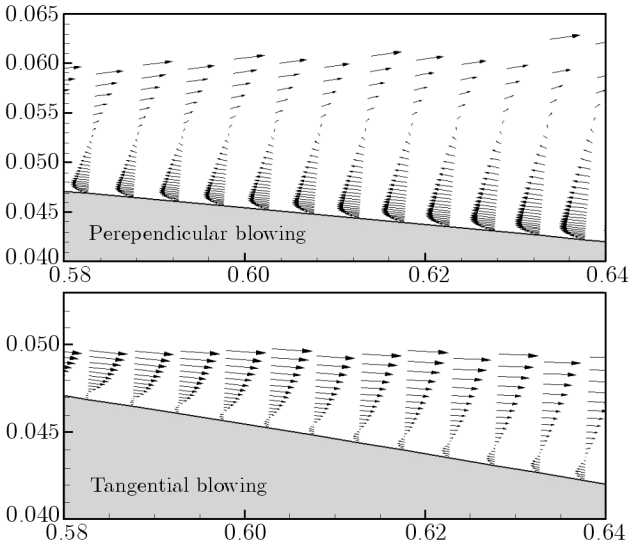

Fig. 15. Comparison between amplitude vectors of the tangential and perpendicular uniform blowing

5. Conclusion

In this study, the effects of tangential and perpendicular blowing flow controls on the NACA 0012 airfoil were numerically analyzed. For this purpose, several parameters including the blowing amplitude and blowing jet width were changed over a wide range, and the following results have been obtained. In the tangential blowing, when the blowing amplitude increases, the lift-to-drag ratio rises as well and the separation point is transferred to the downstream. At the same time, an increase in the blowing amplitude worsens the situation in the perpendicular blowing and makes larger eddies. In the tangential blowing, the greatest increase in the lift-to-drag ratio occurred for the blowing amplitude of 0.5 and the blowing coefficient of 0.01, in which, for the 18 degrees angle of attack, the eddies behind the airfoil decreased. On the other hand, the use of the perpendicular blowing makes the situation worse than no blowing situation (until before stall angle). The results showed that for small angles of attack, the control of flow separation by using the blowing have little effect on improving aerodynamic characteristics. Furthermore, the use of the tangential blowing for the airfoil does not change the stall angle of the airfoil but causes the stall to become slower, while the perpendicular blowing changes the stall angle from 14 to 16 degrees.

The effects of blowing jet widths variations on the airfoil surface were investigated. The results indicate that when the blowing jet width rises, the lift-to-drag ratio increases continuously in the tangential blowing and decreases continuously and quasi-linearly in the perpendicular blowing. In the tangential blowing, the increasing slope of the lift-to-drag ratio decreases from the blowing jet width by 3.5 to 4 percent of the chord length. In this work, the blowing jet width of 3.5 to 4 percent of the chord length for the tangential blowing was selected as an optimal value as smaller blowing widths are more suitable for the perpendicular blowing. Finally, the lift-to--drag ratio was increased by 17 percent for the tangential blowing for the blowing amplitude of 0.5, jet width of 4 percent of the chord length and the angle of attack of 18 degrees.

6. Future works

Although several studies have been carried out experimentally and numerically on suction and blowing flow control, some important parameters like the number of suction/blowing slots, slot arrangements, oscillatory suction/blowing and also synthetic jet parameters have not been fully examined. Laboratory studies on suction and blowing parameters are highly limited.

References

1. Abbott I.H., Von Doenhoff A.E., 1959, *Theory of Wing Sections*, Dover Publications, New York
2. Critzos C.C., Heyson H.H., Boswinkle W., 1955, Aerodynamics characteristics of NACA 0012 airfoil section at angle of attacks from 0° to 180°, *NACA TN*, **3361**
3. Dirlik S., Kimmel K., Sekelsky A., Slomski J., 1992, Experimental evaluation of a 50-percent thick airfoil with blowing and suction boundary layer control, *AIAA Paper*, **92**, 427-445
4. Eppler R., 1990, *Airfoil Design and Data*, Springer, Berlin
5. Flatt J., 1961, The history of boundary layer control research in the United States of America, [In:] *Boundary Layer and Flow Control: its Principles and Application*, G.V. Lachmann (Edit.), New York, Pergamon Press
6. Gad-el-hak M., 2000, *Control Flow: Passive, Active and Reactive Flow Management*, Cambridge University Press, United Kingdom, 25-35
7. Genc M.S., Keynak U., Yapici H., 2011, Performance of transition model for predicting low Re aerofoil flows without/with single and simultaneous blowing and suction, *European Journal of Mechanics B/Fluids*, **30**, 2, 218-235
8. Glauert M.B., 1947, The application of the exact method of aerofoil design,*Aeronautical Research Council, R&M*, **2683**
9. Goodarzi M., Fereidouni R., Rahimi M., 2012, Investigation of flow control over a NACA 0012 airfoil by suction effect on aerodynamic characteristics, *Canadian Journal of Mechanical Sciences and Engineering*, **3**, 3, 102-108
10. Guowei Y., Shanwu W., Ningyu L., Lixian Z., 1997, Control of unsteady vertical lift on an airfoil by leading-edge blowing suction, *ACTA Mechanica Sinica (English Series)*, **13**, 4, 304-312
11. Hazen D.C., 1967, Boundary layer control, *Journal of Fluid Mechanics*, **29**, 200-208
12. Huang L., Huang P.G., LeBeau R.P., 2004, Numerical study of blowing and suction control mechanism on NACA 0012 airfoil, *Journal of Aircraft*, **41**, 5, 1005-1013
13. Jacobs E., Sherman A., 1937, Airfoil section characteristics as affected by variations of the Reynolds number, *NACA Report*, **586**, 227-264
14. Jensch C., Pfingsten, K.C., Radespiel, R., 2010, Numerical investigation of leading edge blowing and optimization of the slot geometry for a circulation control airfoil, *Notes on Numerical Fluid Mechanics and Multidisciplinary Design*, **112**, 183-190
15. Mashud M., Hossain F., 2010, Experimental study of flow separation control of an airfoil by suction and injection, *13th Asian Congress of Fluid Mechanics*, 166-169
16. Menter, F.R., Kuntz, M., Langtry, R., 2003, Ten years of industrial experience with the SST turbulence model, *4th International Symposium on Turbulence, Heat and Mass Transfer*, Turkey
17. Nae C., 1998, Synthetics jets influence on NACA 0012 airfoil at high angle of attacks, *AIAA Papers*, **98-4523**
18. Olejniczak J., Lyrintzis A.S., 1994, Design of optimized airfoils in subcritical flow, *Journal of Aircraft*, **31**, 3, 680-687

19. Ravindran S.S., 1999, Active control of flow separation over an airfoil, *Report of Langley Research Center*, **TM-1999-209838**

20. Rizzetta D.P., Visbal M.R., Stank M.J., 1999, Numerical investigation of synthetic jet flow fields, *AIAA Journal*, **37**, 8, 919-927

21. Rosas C.R., 2005, Numerical simulation of flow separation control by oscillatory fluid injection, Ph.D. Thesis, A&M University, Texas

22. Sahu R., Patnaik B.S.V., 2011, CFD simulation of momentum injection control past a streamlined body, *International Journal of Numerical Methods for Heat and Fluid Flow*, **21**, 8, 960-1001

23. Schlichting H., 1968, *Boundary Layer Theory*, McGraw-Hill, New York, 347-362

24. Seifert A., Darabi A., Wygnansky I., 1996, Delay of airfoil stall by periodic extinction, *Journal of Aircraft*, **33**, 4, 691-698

25. Sheldhal R.E., Klimas P.C., 1981, Aerodynamic characteristics of seven airfoil sections through 180 degrees angle of attack for use in aerodynamic analysis of vertical axis wind tunnel, *Sandia National Laboratories Report*, **SAND80-2114**

26. You D., Moin P., 2008, Active control of flow separation over an airfoil using synthetic jets, *Journal of Fluids and Structures*, **24**, 8, 1349-1357

27. Yousefi K., Saleh R., Zahedi P., 2012, Investigation for increase or decrease the lift and drag coefficient on the airfoil with suction and blowing, *International Conference on Mechanical Engineering and Advanced Technology*, Iran

28. Yousefi K., Saleh R., Zahedi P., 2013a, Numerical investigation of suction and length of suction jet on aerodynamic characteristics of the NACA 0012 airfoil, *International Journal of Materials, Mechanics and Manufacturing*, **1**, 2, 136-142

29. Yousefi K., Saleh R., Zahedi P., 2013b, Numerical study of flow separation control by tangential and perpendicular blowing on the NACA 0012 airfoil, *International Journal of Engineering*, **7**, 1, 10-24

Manuscript received February 4, 2013; accepted for print August 12, 2013